Supplementary Information

Optimal icosahedral copper-based bimetallic clusters for the selective electrocatalytic CO_2 conversion to one carbon products

Azeem Ghulam Nabi,*[1,2,3,5] Aman ur Rehman[2,4], Akhtar Hussain,[5] Gregory A. Chass [1,6,7] and Devis Di Tommaso,*[1]

[1] Department of Chemistry, School of Physical and Chemical Sciences, Queen Mary University of London, Mile End Road, London, E1 4NS, United Kingdom
[2] Department of Physics and Applied Mathematics, Pakistan Institute of Engineering and Applied Sciences, P. O. Nilore, Islamabad, Pakistan
[3] Department of Physics, University of Gujrat, Jalalpur Jattan Road, Gujrat, Pakistan
[4] Department of Nuclear Engineering, Pakistan Institute of Engineering & Applied Sciences, P.O. Nilore, Is-lamabad, 45650, Pakistan
[5]Theoretical Physics Division, Pakistan Institute of Nuclear Engineering & Technology (PINSTECH), Islamabad , Pakistan
[6] Department of Chemistry, McMaster University, Hamilton, Ontario, L8S 4L8, Canada
[7] Faculty of Land and Food Systems, The University of British Columbia, Vancouver BC, V6T1Z4, Canada

TABLE S1. The energies (E), zero-point energies (ZPE), and entropies (S) of H_2(g), CO_2(g) and CO(g), and H_2O. The entropies of H_2(g), CO_2(g) and CO(g) were calculated at 1 atm. The entropy of H_2O (g=l) was calculated at 0.035 atm, which corresponds to the vapor pressure of liquid water.

Gas Phase	**E**	**ZPE**	***$C_p dT$***	**TS**	**ΔG**
H_2	-6.71	0.27	0.09	-0.41	-6.76
H_2O	-14.2	0.56	0.1	-0.65	-14.19
CO(g)	-14.43	0.13	0.09	-0.59	-14.8
CO_2	-22.96	0.27	0.1	-0.65	-23.24

Table S2. The atomic, covalent and Van der Waals radii, the electronegativity difference, electronic configuration, and calculated value of segregation energies (in eV).

Atomic Symbol	**Radius [Å]**[1][2]					**Segregation Energy (eV)**	
	Atomic	**Covalent**	**Van-der-Waals**	**ΔE_N (eV)**	**Electronic Configuration**	**CN6**	**CN8**
Cu	1.45	1.38	1.40	0.00	$4s^1 3d^{10}$		
Ag	1.65	1.53	1.72	0.03	$5s^1 4d^{10}$	-1.46	-1.53
Cd	1.61	1.48	1.58	0.21	$5s^2 4d^{10}$	-2.50	-2.60
Pd	1.69	1.31	1.63	0.30	$4p^6 4d^{10}$	-0.46	-0.59
Pt	1.77	1.28	1.75	0.38	$5d^9 6s^1$	-0.20	-0.38
Zn	1.42	1.31	1.39	0.25	$4s^2 3d^{10}$	-0.57	-0.68

[1] S. Alvarez, "A cartography of the van der Waals territories," *Dalt. Trans.*, vol. 42, no. 24, pp. 8617–8636, 2013, doi: 10.1039/c3dt50599e.

[2] B. Cordero *et al.*, "Covalent radii revisited," *J. Chem. Soc. Dalt. Trans.*, no. 21, pp. 2832–2838, 2008, doi: 10.1039/b801115j.

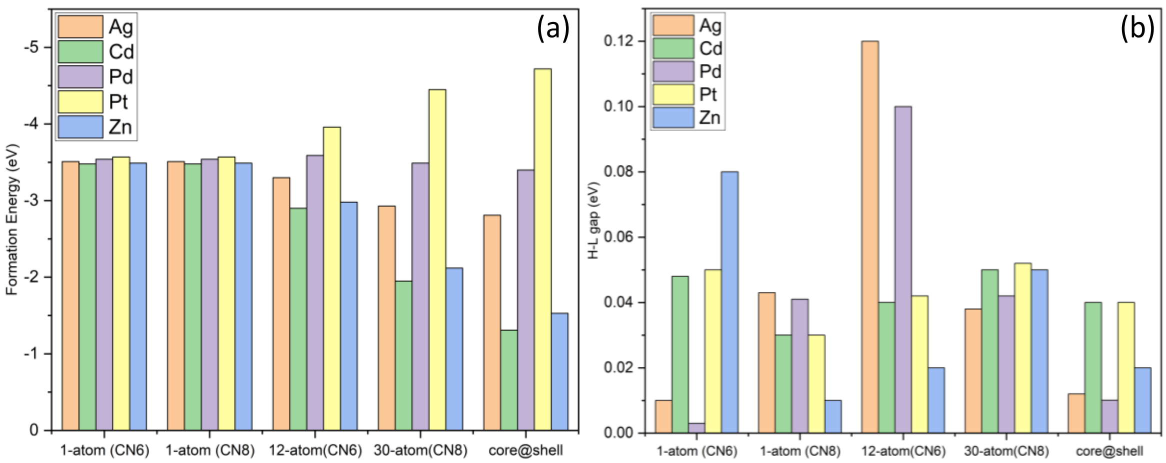

Figure S1. (a) The binding energy and **(b)** HOMO-LUMO (H-L) gap of Cu-M clusters with increasing doping concentration.

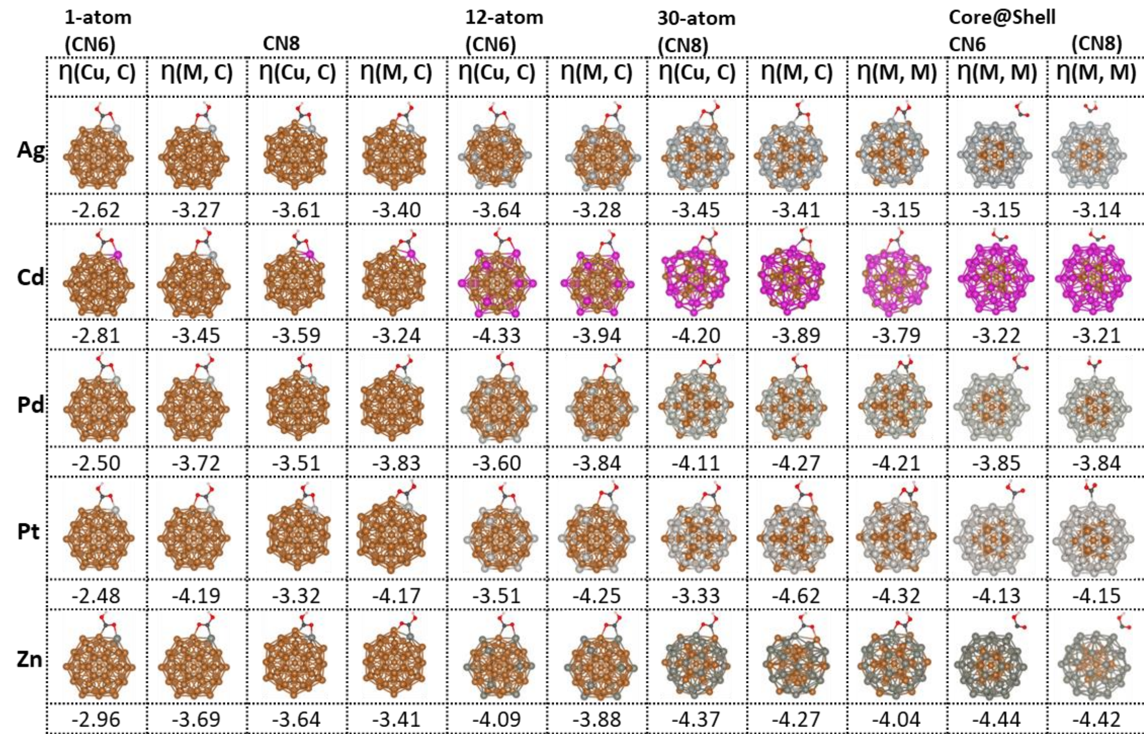

Figure S2. The structure and adsorption energies (in eV) of COOH adsorbed on the Cu-M clusters.

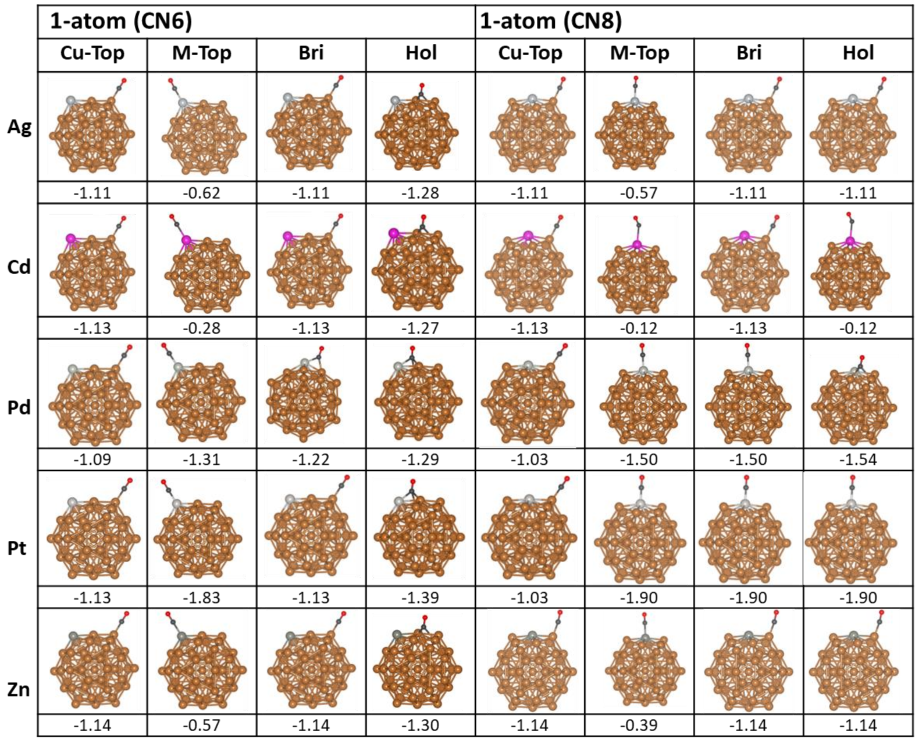

Figure S3. The structure and adsorption energies (in eV) of CO adsorbed on the $Cu_{54}M$ clusters with CN6 and CN8 nano-catalysts.

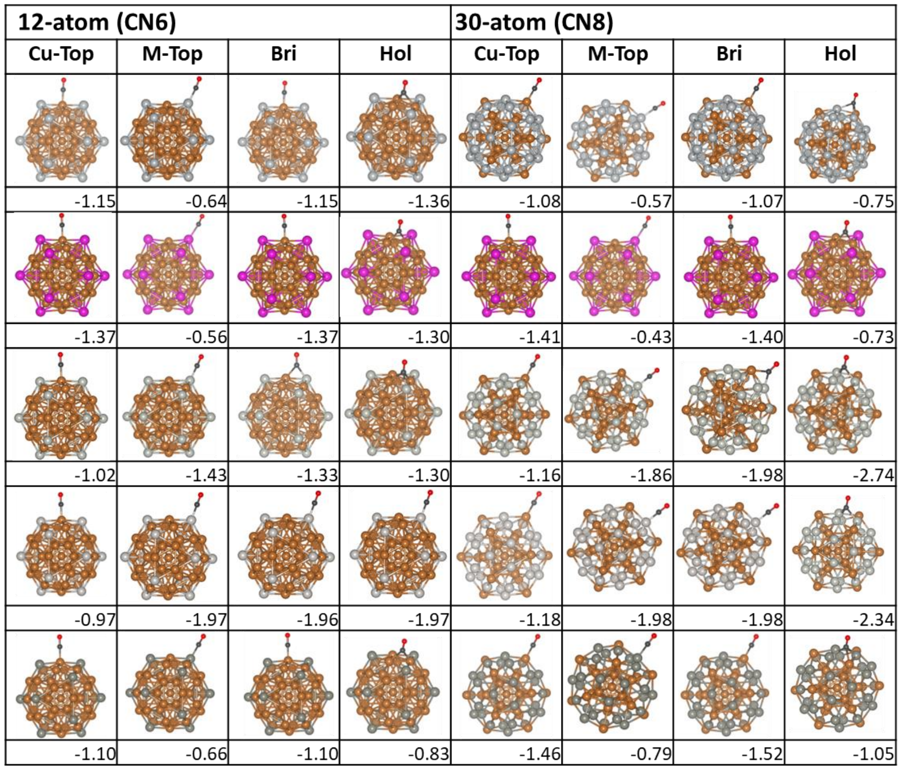

Figure S4. The structure and adsorption energies (in eV) of CO on the $Cu_{43}M_{12}$ and $Cu_{25}M_{30}$ clusters.

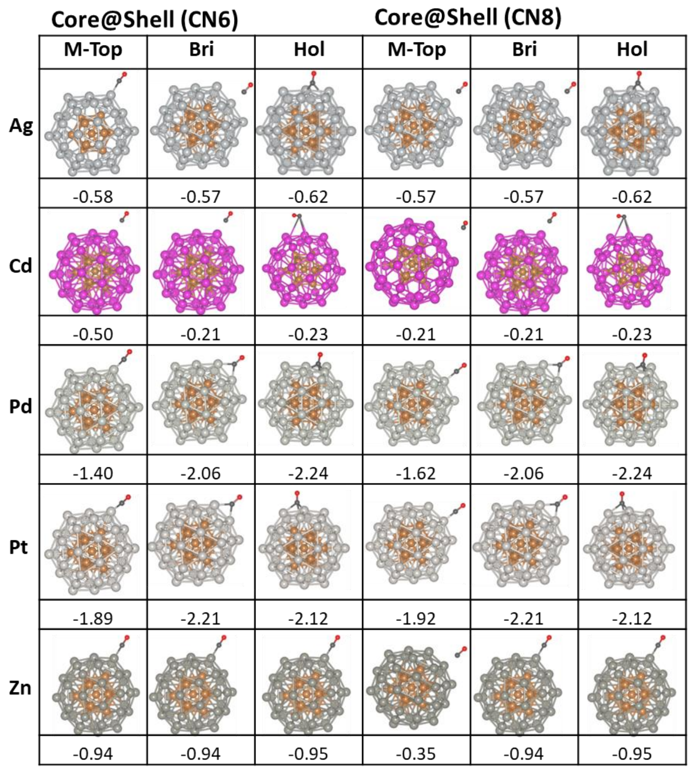

Figure S5. The structure and adsorption energies (in eV) of CO on the $Cu_{43}M_{12}$ and $Cu_{25}M_{30}$ clusters.

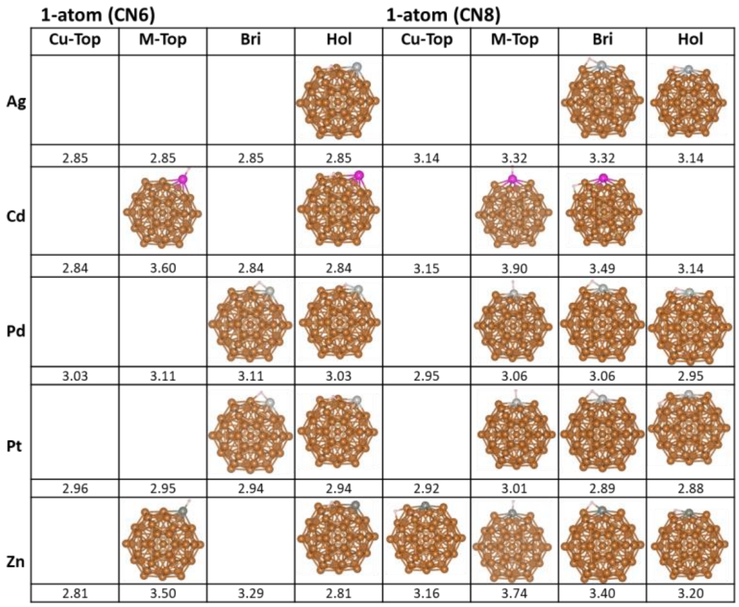

Figure S6. The structure and adsorption energies of H adsorbed on the $Cu_{43}M_{12}$ and $Cu_{25}M_{30}$ clusters at the Top, Hollow and Bridge positions.

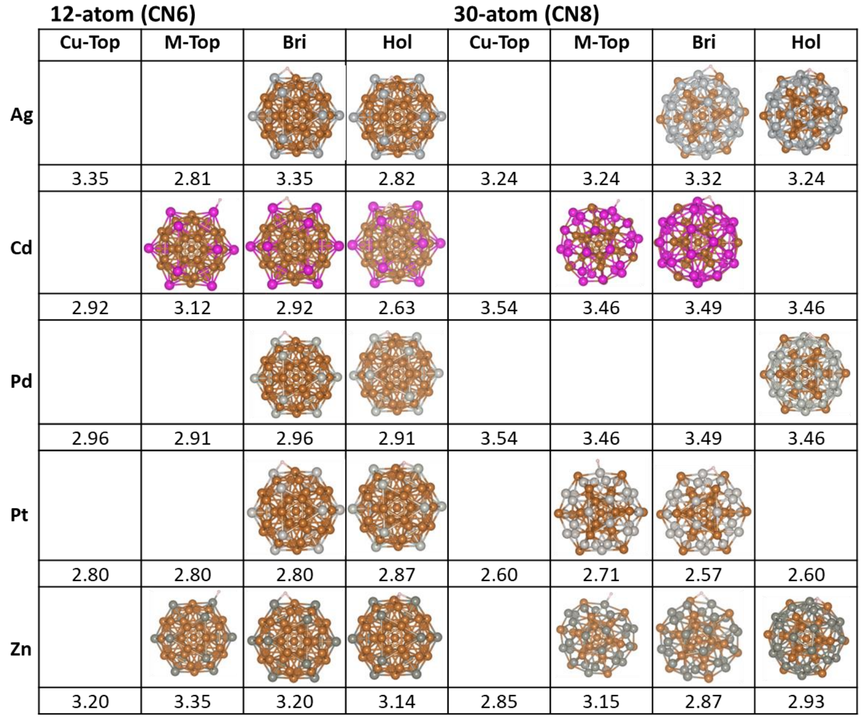

	12-atom (CN6)				30-atom (CN8)			
	Cu-Top	M-Top	Bri	Hol	Cu-Top	M-Top	Bri	Hol
Ag	3.35	2.81	3.35	2.82	3.24	3.24	3.32	3.24
Cd	2.92	3.12	2.92	2.63	3.54	3.46	3.49	3.46
Pd	2.96	2.91	2.96	2.91	3.54	3.46	3.49	3.46
Pt	2.80	2.80	2.80	2.87	2.60	2.71	2.57	2.60
Zn	3.20	3.35	3.20	3.14	2.85	3.15	2.87	2.93

Figure S7. The structure and adsorption energies of H adsorbed on the $Cu_{43}M_{12}$ and $Cu_{25}M_{30}$ clusters at Top, Hollow and Bridge positions.

	Core@Shell (CN6)			Core@Shell (CN8)		
	M-Top	Bri	Hol	M-Top	Bri	Hol
Ag		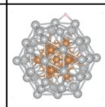	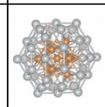		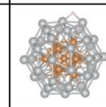	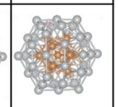
	3.52	3.52	3.40	3.53	3.51	3.41
Cd	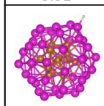	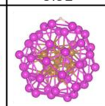			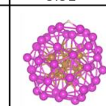	
	4.10	4.10	4.10	4.10	4.10	4.10
Pd		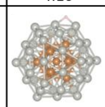	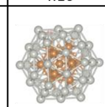		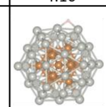	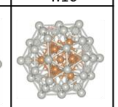
	2.88	2.88	2.72	2. 85	2.82	2.73
Pt		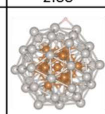	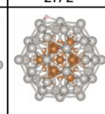	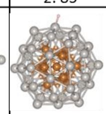	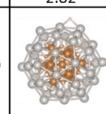	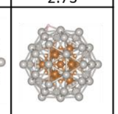
	2.74	2.74	2.81	2.74	2.75	2.82
Zn	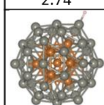			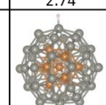	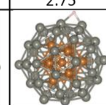	
	2.69	2.69	2.68	2.68	2.67	2.69

Figure S8. The structures and adsorption energies of H adsorbed on the core@shell clusters at Top, Hollow and Bridge positions.

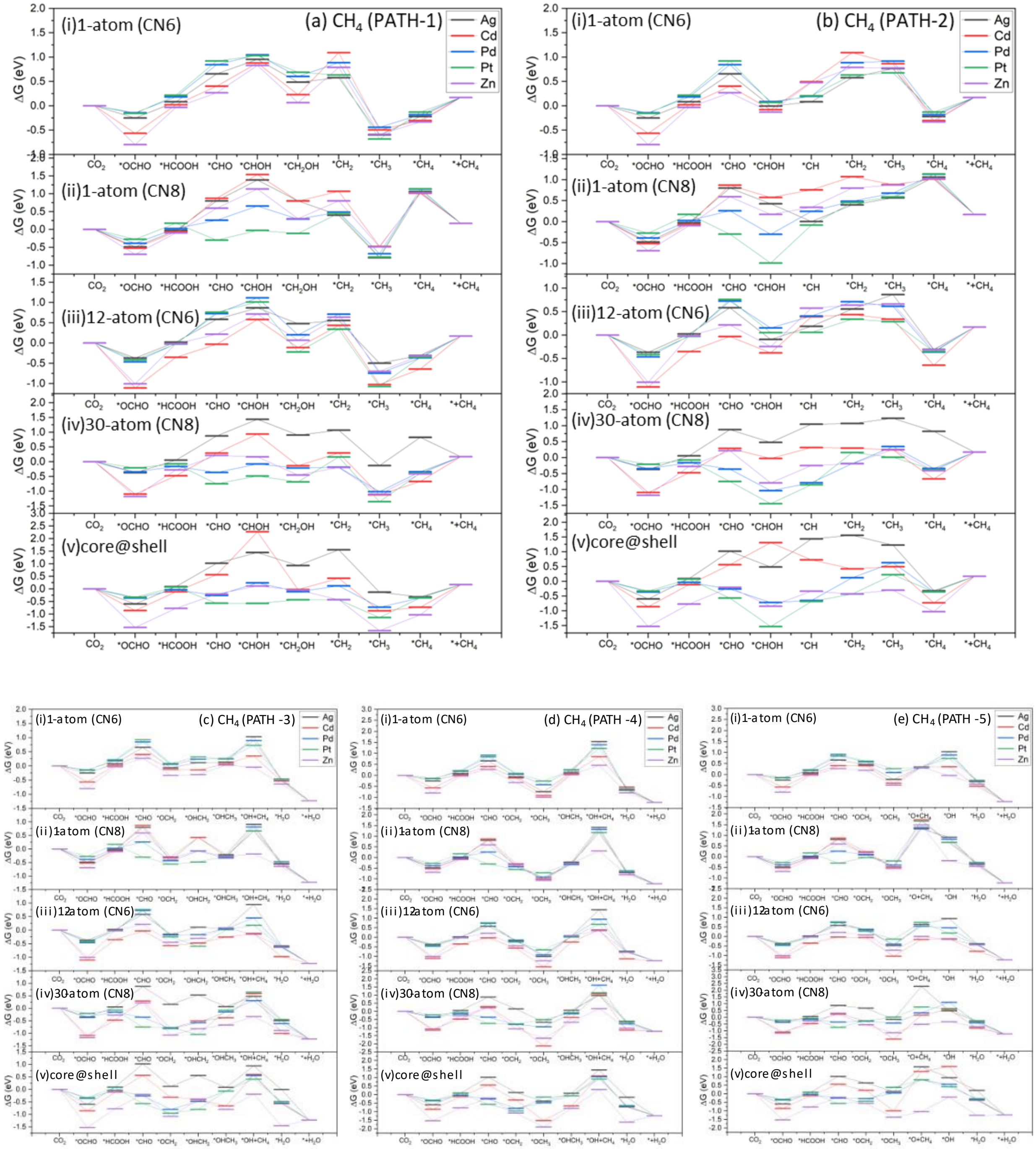

Figure S9. Gibbs free energy diagram for the CH_4 formation on CuM clusters along pathways 1 to 5: **(1)** $*CHO \rightarrow *CHOH \rightarrow *CH \rightarrow *CH_2 \rightarrow *CH_3 \rightarrow * + CH_4$; **(2)** $*CHO \rightarrow *CHOH \rightarrow *CH_2OH \rightarrow *CH_2 \rightarrow *CH_3 \rightarrow * + CH_4$; **(3)** $*CHO \rightarrow *OCH_2 \rightarrow *OHCH_2 \rightarrow *OHCH_3 \rightarrow *OH + CH_4 \rightarrow * + H_2O$; **(4)** $*CHO \rightarrow *OCH_2 \rightarrow *OCH_3 \rightarrow *OHCH_3 \rightarrow *OH + CH_4 \rightarrow * + H_2O$; **(5)** $*CHO \rightarrow *OCH_2 \rightarrow *OCH_3 \rightarrow *O + CH_4 \rightarrow *OH \rightarrow * + H_2O$.

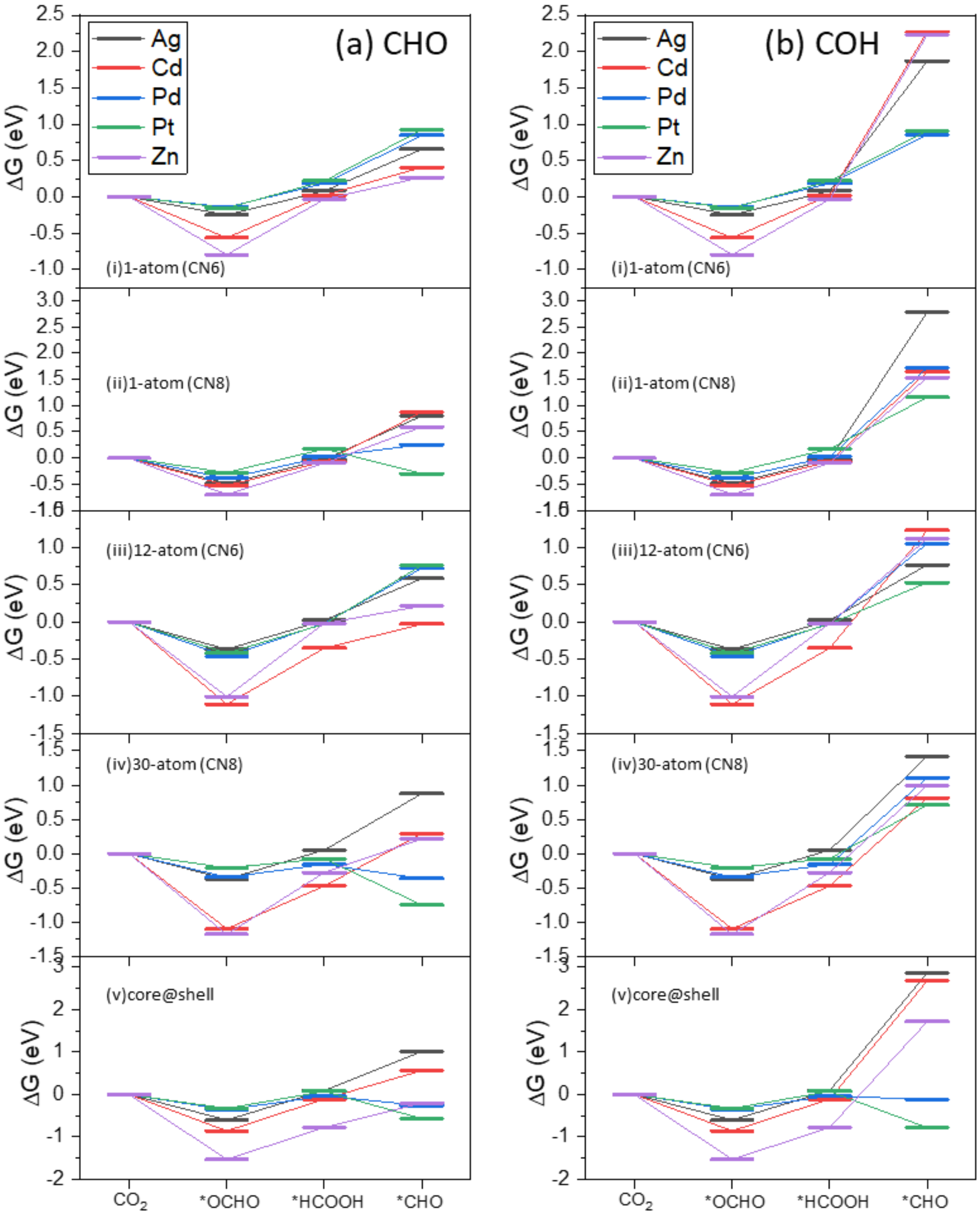

Figure S10. Gibbs free energy diagram for CHO **(a)** and COH **(b)** formation on CuM clusters.